

M agnetic O rdering in the Spin-Ice C andidate $\text{H}_2\text{Ru}_2\text{O}_7$ C . R . W ieb e,^{1,2} J . S . G ardner,^{3,4} S . J . K im,¹ G . M . L uke,¹ A . S . W ills,⁵
B . D . G aulin,¹ J . E . G reedan,⁶ I . S wainson,⁷ Y . Q iu,^{4,8} and C . J ones⁴¹D epartm ent of Physics and A stron om y, M cM aster University, H am ilton, Ontario L8S 4M 1, Canada²D epartm ent of Physics, Colum bia University, New York, New York 10027, USA³D epartm ent of Physics, Brookhaven National Laboratory, Upton, New York, 11973-5000, USA⁴N IST Center for Neutron Research, Gaithersburg, Maryland, 20899-5682, USA⁵D epartm ent of Chem istry, University College London, 20 Gordon Street, London, W C 1H 0AJ, UK⁶D epartm ent of Chem istry, M cM aster University, H am ilton, Ontario L8S 4M 1, Canada⁷NPMR, NRC, Chalk River, Ontario K0J 1J0, Canada⁸D epartm ent of M aterials Science and Engineering,
University of M aryland, College Park, M aryland, 20742, USA

(D ated: M arch 22, 2024)

Neutron scattering m easurem ents on the spin-ice candidate m aterial $\text{H}_2\text{Ru}_2\text{O}_7$ have revealed two m agnetic transitions at $T = 95$ K and $T = 1.4$ K to long-range ordered states involving the Ru and H o sublattices, respectively. Between these transitions, the H o^{3+} m om ents form short-ranged ordered spin clusters. The internal eld provided by the ordered $S = 1$ Ru^{4+} m om ents disrupts the fragile spin-ice state and drives the H o^{3+} m om ents to order. W e have directly m easured a slight shift in the H o^{3+} crystal eld levels at 95 K from the Ru ordering.

PACS num bers: 71.70.Ch, 75.10.-b, 75.25.+z

Frustration, a condition which describes the inability of a system to satisfy all of its individual interactions simultaneously,[1] has become an important concept in the realm of condensed matter physics, being applicable to a wide range of phenomena such as high- T_c superconductors, liquid crystal phase transitions, and protein folding. A renewed interest in geometrically frustrated magnets has resulted from this general interest in frustration and the discovery of new magnetic ground states. One of these new states is the spin-ice, which occurs on the pyrochlore lattice of corner sharing tetrahedra with weak ferromagnetic coupling between rare-earth ions subject to strong axial crystal elds.[2] In particular, the h111 anisotropy of these sites promotes a "two-in, two-out" low temperature spin arrangement upon each tetrahedron, which is stabilized by dipolar interactions.[3] The resulting ground state has a macroscopic entropy associated with the many ways that each tetrahedron can satisfy this condition independently of the other tetrahedra.[4] The short-ranged order of the spins on each tetrahedra maps onto the problem of proton ordering in water ice. Pauling first realized the significance of the specific heat anomaly at the ice transition temperature as being due to the disorder at each oxygen site.[5] An excellent agreement has been found between the spin ice model and physical properties including magnetization,[6], [7] specific heat,[4] and neutron scattering experiments [8] of the three spin ices, $\text{Dy}_2\text{T i}_2\text{O}_7$, $\text{H}_2\text{T i}_2\text{O}_7$ and $\text{H}_2\text{Sn}_2\text{O}_7$.

Recently, a new spin-ice candidate has been discovered by Bensalet al. - $\text{H}_2\text{Ru}_2\text{O}_7$. [9] Whereas other spin ices of the form $\text{A}_2\text{B}_2\text{O}_7$ only have one magnetic species on the A site, in $\text{H}_2\text{Ru}_2\text{O}_7$ both A and B sites are magnetic: H o^{3+} $J = 8$ spins and Ru^{4+} $S = 1$ spins. Previous studies

on the closely related pyrochlores in the series $\text{R}_2\text{Ru}_2\text{O}_7$ ($\text{R} = \text{Y}, \text{Nd}$) have revealed that the Ru^{4+} m om ents order at higher temperatures ($T = 100$ K). $\text{H}_2\text{Ru}_2\text{O}_7$ shows an anomaly in the magnetic susceptibility which agrees with these findings and suggests that the Ru^{4+} m om ents order at 95 K. [10] However, this claim has not been verified until this work. This letter details the study of $\text{H}_2\text{Ru}_2\text{O}_7$ by neutron scattering to determine if the Ru^{4+} m om ents order and, if so, to investigate the effect of the internal eld on the H o^{3+} m om ents, which dominate the magnetic response. W e will show that the Ru^{4+} m om ents do order at 95 K into a spin-ice like state of their own, while magnetic short range correlations develop between the H o^{3+} m om ents as the temperature is lowered further. The internal eld associated with the Ru^{4+} sublattice appears to be enough of a perturbation upon the H o^{3+} ions to induce a low temperature transition to a long-range ordered state at 1.4 K which is not seen down to 50 m K of the other spin-ices.

W e have made 20g of $\text{H}_2\text{Ru}_2\text{O}_7$ powder with less than 1% excess Ru metal as determined by X-ray and neutron diffraction. The magnetic properties were measured between 2 K and 600 K using a commercial SQUID magnetometer. Elastic neutron diffraction measurements were performed with 2.37 and 2.0775 Å neutrons at Chalk River and NIST respectively from room temperature to 100 m K. Inelastic neutron scattering was performed using various wavelengths (3 to 9 Å) at the Disk Chopper Spectrometer (DCS) at NIST. [11] Symmetry analysis calculations were carried out using the program SARA-H-Representational Analysis. [12] Rietveld refinements were done using Fullprof. [13]

High temperature susceptibility data was fitted to the Curie Weiss law and a Weiss temperature of $-3(2)$ K was

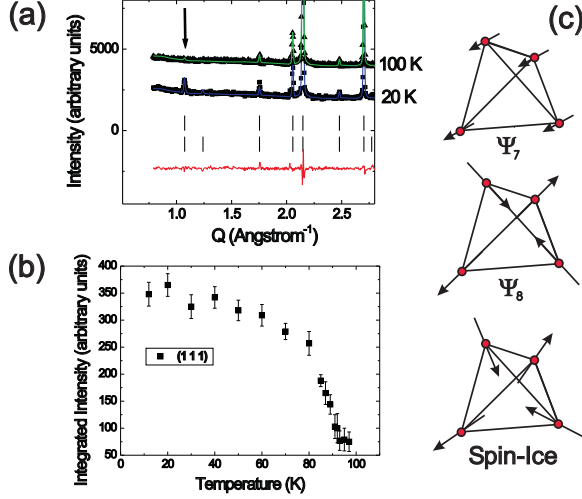


FIG. 1: (a) Neutron scattering with 2.37 Å neutrons at $T = 100$ K and $T = 20$ K. The ticks are to the crystal structure of $\text{Ho}_2\text{Ru}_2\text{O}_7$ (upper tick marks) and a magnetic structure (lower tick marks) described in the text. The residual of the 20 K fit is at the bottom of the plot ($R_p = 1.99$, $R_{wp} = 2.69$, $\chi^2 = 2.02$ at 100 K; $R_p = 2.82$, $R_{wp} = 3.73$, $R_{mag} = 40.9$, $\chi^2 = 3.73$ at 20 K). (b) The integrated intensity of the magnetic (111) reflection (as indicated in figure 1(a)). (c) Ψ_7 and Ψ_8 of the IR, Ψ_9 , and the spin-ice state which arises from equal proportions of these basis vectors.

determined. This is in agreement with $-4(0.5)$ K [9] found by Bensalet al. and is indicative of weak antiferromagnetic coupling. Assuming that the response is largely due to holmium, the Curie constant corresponds to an effective moment of $9.29(3) \mu_B$, just short of the expected value for the $\text{Ho}^{3+} 5f_8$ ion of $10.6 \mu_B$ and again in agreement with Bensalet al.

Below 95 K, where a small field-cooled/zero-field-cooled divergence in the susceptibility data is seen, magnetic Bragg peaks appear which can be indexed with a $k = 0$ propagation vector. These peaks are situated on top of diffuse magnetic scattering at low Q , which grows in intensity as one cools (see figure 2). This diffuse scattering is attributed to regions of short-ranged magnetic order (SRO) from the Ho^{3+} species. Spin-ices have a characteristic diffuse scattering profile which is indicative of the ferromagnetic SRO (i.e. an accumulation of scattering about $Q = 0$ [14]). However, an unambiguous determination of the nature of this scattering requires further study, preferably on single crystals. A slight broadening of the magnetic Bragg peaks with respect to the nuclear, and the reduced ordered moment with respect to expected $S = 1$ value ($1.2(2) \mu_B$ as compared to $2 \mu_B$) indicates that not all of the Ru^{4+} moments are ordered. From the (111) magnetic peak, one can estimate the correlation length of the Ru^{4+} ordered spins to be ~ 250 Å,

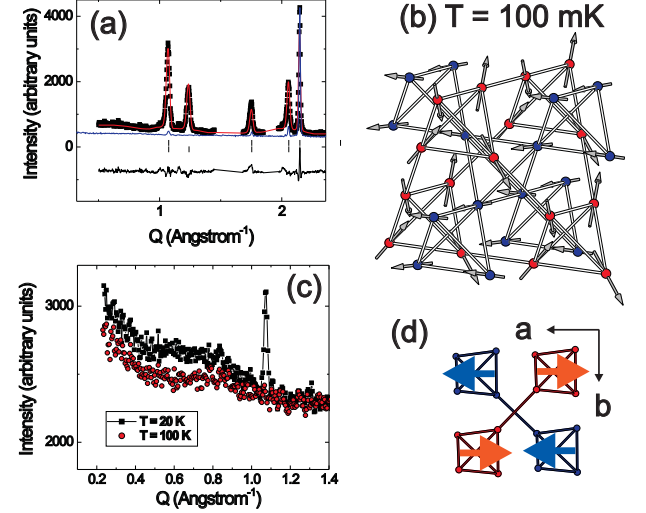


FIG. 2: (a) The diffraction data, fit (red line) and residual (black line) for 2.0775 Å neutrons at 100 mK. The upper tick marks are for the crystal structure and the lower for the magnetic ($R_p = 6.06$, $R_{wp} = 7.85$, $R_{mag} = 8.62$, $\chi^2 = 4.35$). The 20 K neutron data (blue line) is normalized to the (222) predominantly nuclear reflection. (b) The magnetic structure of the Ru moments (blue) and Ho moments (red) at 100 mK. For clarity, only a portion of the unit cell is shown, and the ordered moments are not drawn to scale. (c) Diffraction data with 2.37 Å neutrons at $T = 20$ K and $T = 100$ K, showing an intermediate state of SRO Ho^{3+} above 1.4 K. (d) The magnetic structure at 100 mK can be thought of as a nearly collinear ferromagnet (Ru sites, in blue) and a spin-ice like state (Ho sites, in red) upon the different sublattices. The net moment cancels from one sublattice to the next along one crystallographic direction.

or about 25 unit cells. Further study of their ordering is not possible as the diffuse scattering is dominated by that of the much larger Ho^{3+} moment.

The magnetic contribution to the powder neutron diffraction spectrum of $\text{Ho}_2\text{Ru}_2\text{O}_7$ below 95 K can be well described by ordering of the Ru^{4+} moments according to the irreducible representation Ψ_9 of the space group $Fd\bar{3}m$. [16] This irreducible representation has 6 associated basis vectors and may be thought of as involving a ferromagnetic structure along the a -axis, Ψ_7 , an orthogonal antiferromagnetic structure, Ψ_8 , and those related by alternative choices of the lattice axis (see figure 1). As neutron diffraction from a powder cannot distinguish the orientation of these structures with respect to the cubic axes, we restricted our analysis to the Hilbert space defined by Ψ_7 and Ψ_8 . We note that equal proportions of Ψ_7 and Ψ_8 correspond to a spin ice state with the propagation vector $k = 0$. At 20 K the ordering is found to be $0.881 \Psi_7 + 0.774 \Psi_8$ indicating that the Ru^{4+} moments order with a spin ice-like local structure. It is

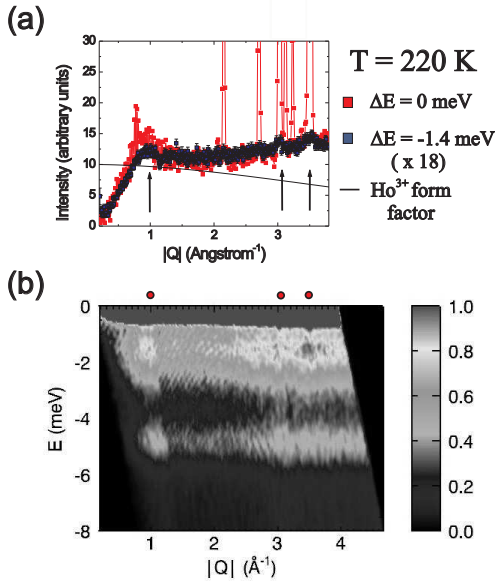


FIG. 3: (a) Integrated neutron scattering data at energy transfers of 0 meV and -1.4 meV and at 220 K (with a width of 0.6 meV) with the DCS and neutrons of $\lambda = 3$ Å. The positions of the (111), (422) and (440) reflections are noted, as well as the Ho^{3+} form factor. (b) Neutron scattering contour plot at $T = 220$ K, showing dispersionless features at -1.4 meV and -4.8 meV. [15]

convenient to characterize these structures according to the angle, θ , that the moments make with the uncompensated ferromagnetic component, in this case the a -axis. Thus a collinear ferromagnet would have an angle of 0°, the state γ_8 an angle of 90°, and spin-ice an angle of $109/2 = 54.5^\circ$. A value of $\theta = 41^\circ$ for the Ru moments indicates that the structure is more ferromagnetically collinear than the pure spin-ice state. The ordered component ($1.2(2)$ μ_B) is within error of the previous determinations of 1.36 μ_B and 1.18 μ_B for the ordered moments in $\text{Y}_2\text{Ru}_2\text{O}_7$ and $\text{Nd}_2\text{Ru}_2\text{O}_7$ respectively, but the proposed magnetic structures are different. [10] A recent neutron scattering study of $\text{Er}_2\text{Ru}_2\text{O}_7$ has revealed a planar structure involving Er^{3+} and Ru^{4+} ordered moments below 90 K, however we see no evidence for Ho^{3+} ordering at 90 K in $\text{Ho}_2\text{Ru}_2\text{O}_7$. [18]

Below 1.4 K, additional Bragg peaks appear in the diffraction data (figure 2). The data could only be well fitted by assuming that both the Ru^{4+} and Ho^{3+} moments order according to the representation γ_9 . Unlike the 20 K data, contributions from both Ru and Ho sublattices were required, and the final ordered moments are 1.8(6) μ_B on the Ru and 6.3(2) μ_B on the Ho. The Ru^{4+} moments seem to be enhanced, but they are still within error of the 20 K values. The refined moments were oriented at 10° and 73° with respect to the uncompensated component indicating that the Ho^{3+} ordering reduced

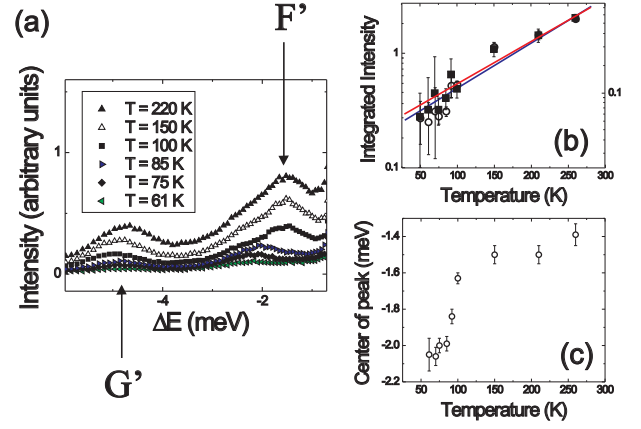


FIG. 4: (a) Integrated scans from $Q = 0.6$ Å $^{-1}$ to 4.0 Å $^{-1}$ at 220 K. Note the crystal field transitions, indicated by F' and G' . (b) Integrated intensities of the crystal field peaks, as fitted to gaussians, as a function of temperature. The open circles (blue) belong to the left scale (F' transitions) and the closed squares (red) belong to the right (G' transitions). (c) Shift of the center of the gaussian peak for F' transitions.

the frustration of the Ru^{4+} moments and increased their collinearity. The Ho^{3+} moments themselves are more antiferromagnetic than ferromagnetic (with more γ_8 character than γ_7). Interestingly, the Ru^{4+} moments orient themselves such that they cancel one component of the Ho^{3+} spins, which in our definition is the a -axis. In the a - b plane, one can think of the two sublattices as being antiferromagnetically aligned, as shown in figure 2(d).

Bensalet al. concluded that in $\text{Ho}_2\text{Ru}_2\text{O}_7$, the long-range dipolar interactions among the Ho^{3+} spins do not destroy the degeneracy of the spin-ice state, since the condition imposed by den Hertog and Gingras, [3] $J_{\text{eff}} / D_{\text{NN}}$ (effective nearest neighbor energy scale) / D_{NN} (dipolar energy scale) > 0.09 , is satisfied. However, we note that this is only true if the Weiss constant is adjusted for Van Vleck paramagnetism and demagnetization factors as found by Bramwell et al. for $\text{Ho}_2\text{Ti}_2\text{O}_7$. [19] More precise measurements are needed on single crystals of $\text{Ho}_2\text{Ru}_2\text{O}_7$ to determine the Weiss constant (and thus, J_{eff}). Our experiments clearly show that the Ho^{3+} moments do order, and do not form the spin-ice state.

High energy resolution inelastic neutron scattering was performed on 20 g of sample on the DCS. A representative spectrum at 220 K is shown in figure 3(b). The dispersionless features at finite energy transfer are a result of transitions between crystal field levels at higher energies than those measured on the DCS ($E > 10$ meV). Figure 3(a) shows that these excitations do not follow the form factor as predicted from isolated Ho^{3+} moments, but they are modulated in Q in a manner which follows the diffuse scattering seen at $E = 0$ meV. The scat-

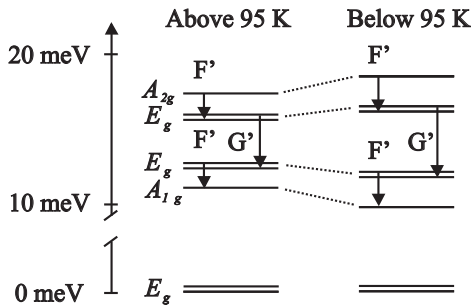


FIG. 5: Schematic of the crystal field levels in $\text{H}_2\text{Ru}_2\text{O}_7$ (adapted from Rosenkranz et al.[21]). The transitions F' and G' are noted. As the Ru^{4+} moments order, the crystal fields are split slightly. The schematic is not to scale and the splitting is exaggerated for clarity.

tering tends to be peaked at values which correspond to the (111), (422) and (440) reflections, which are ferromagnetic points within the unit cell. This indicates that the Ho^{3+} spins have net ferromagnetic interactions, which is expected for a spin-ice, and do not interact as isolated units. Future work is needed to elucidate the Q -dependence of this data. It is unusual that such correlations are seen at high temperatures, but not unprecedented, as in the case of $\text{Tb}_2\text{Ti}_2\text{O}_7$, which has short-ranged correlations up to at least 100 K.[20]

Using $\text{H}_2\text{Ru}_2\text{O}_7$ as a model and the notation adopted by Rosenkranz [21], one can discuss the transitions seen in figure 4. Transitions are observed at $E = -1.5$ meV (denoted F') and -4.8 meV (denoted G'). Fitting these peaks to gaussian functions, the temperature dependence can be plotted (see figure 4(b)), and exponential behavior is noted with activation energies of 105(4) K (F' transition) and 113(9) K (G' transition). This corresponds to a separation of 10 meV from the ground state.

There is a clear shift in the center of these peaks as a function of temperature. Figure 4(c) shows an increase in separation between the levels below 95 K. The Ru^{4+} ordering induces a small internal field, which provides a Zeeman-like splitting of the Ho^{3+} levels as illustrated in figure 5. Since there is a small ferromagnetic component to the Ru^{4+} ordering, this is not a surprising result. It does show, however, that the Ru^{4+} ordering has a measurable effect upon the Ho^{3+} crystal fields. Although there is a short-ranged ordered state on the Ho^{3+} sites well above 1.4 K, it appears that the Ru^{4+} ordering is enough of a perturbation of the fragile spin-ice state to induce ordering upon the Ho^{3+} site and drive the system to order. It has been suggested that the dominant interaction is dipolar at low temperatures, with an interaction energy scale of 0.24 K.[9] This is reasonable to assume, given the localized nature of the f electrons of Ho^{3+} . Superexchange pathways are likely to be complicated between the two magnetic sublattices.

In conclusion, we find that $\text{H}_2\text{Ru}_2\text{O}_7$ is not a spin-ice, and has two magnetic ordering transitions; with Ru^{4+} and Ho^{3+} ordering at 95 K and 1.4 K, respectively. The magnetic properties of the rare earth pyrochlores are the result of a delicate balance between single ion anisotropy, exchange, and dipolar coupling.[2] Although other rare earth pyrochlores such as $\text{Er}_2\text{Ti}_2\text{O}_7$ [22] and $\text{Gd}_2\text{Ti}_2\text{O}_7$ [23] order, it is found that the corresponding structures vary considerably due to the roles played by these complicated interactions. We suggest that the Ho^{3+} ordering found in $\text{H}_2\text{Ru}_2\text{O}_7$ is due to the small internal field produced by the Ru^{4+} ordering. The subtle change in the Ho^{3+} crystal field scheme that we have observed is convincing evidence for this hypothesis.

C. R. Wiebe would like to acknowledge support from NSERC in the form of a PDF. The authors would like to thank the financial support of NSERC, EMK, and CIAR. This work utilized facilities supported in part by the National Science Foundation under Agreement No. DMR-0086210. Work at Brookhaven is supported by the Division of Material Sciences, U. S. Department of Energy under contract DE-AC02-98CH10996. The authors are also grateful for the technical support of the NPMR staff at Chalk River, and Ross Erwin at NIST.

Electronic address: wiebecr@mcmaster.ca

- [1] J. E. Greedan, Chem. Mater. 10, 3058 (1998).
- [2] S. T. Bramwell et al., Science 294, 1495 (2001).
- [3] B. C. den Hertog et al., Phys. Rev. Lett. 84, 3430 (2000).
- [4] A. P. Ramirez et al., Nature 399, 333 (1999).
- [5] L. Pauling, J. Am. Chem. Soc. 57, 2680 (1935).
- [6] A. L. Cornelius et al., Phys. Rev. B 64, 060406 (2001).
- [7] O. A. Petrenko et al., Phys. Rev. B 68, 012406 (2003).
- [8] S. T. Bramwell et al., Phys. Rev. Lett. 87, 047205 (2001).
- [9] C. Bensalet et al., Phys. Rev. B 66, 052406 (2002).
- [10] M. Ito et al., J. Phys. Chem. Solids 62, 337 (2001).
- [11] J. R. D. Copley et al., Chem. Phys. 292, 477 (2003).
- [12] A. S. Wills, Physica B 276, 680 (2000), program available from [ftp://ftp.ill.fr/pub/dif/sarah/](http://ftp.ill.fr/pub/dif/sarah/)
- [13] J. Rodriguez-Carvajal, Physica B 192, 55 (1993).
- [14] H. Kadowaki et al., Phys. Rev. B 65, 144421 (2002).
- [15] Data analysis was completed with DAVE, which can be obtained at <http://www.nsnr.nist.gov/dave/>.
- [16] We follow the labeling scheme used by Kovalev in Ref.17.
- [17] O. V. Kovalev, Representations of the Crystallographic Space Groups Edition 2 (Gordon and Breach Science Publishers, Switzerland, 1993).
- [18] N. Taira et al., J. Solid State Chem. 176, 165 (2003).
- [19] S. T. Bramwell et al., J. Phys. Cond. Matt. 12, 483 (2000).
- [20] J. S. Gardner et al., Phys. Rev. B 64, 224416 (2001).
- [21] S. Rosenkranz et al., J. Appl. Phys. 87, 5914 (2000).
- [22] J. D. M. Champion et al., Phys. Rev. B 68, 020401(R) (2003).
- [23] J. D. M. Champion et al., Phys. Rev. B 64, 140407(R) (2001).